Journal of Environmental Chemical Engineering 12 (2024) 111848

Contents lists available at ScienceDirect

Journal of Environmental Chemical Engineering

journal homepage: www.elsevier.com/locate/jece

Reclamation of impacted urban phreatic water through nanofiltration technology: Insight on natural organic matter removal by fluorescence spectroscopy

Misael Abenza [a,*], Julio López [a], José Luis Beltrán [b], José Luis Cortina [a,c], Joan de Pablo [a,d], Enric Vázquez-Suñé [e], Oriol Gibert [a]

[a] Department of Chemical Engineering and Barcelona Research Center for Multiscale Science and Engineering, EEBE, Universitat Politècnica de Catalunya (UPC)-BarcelonaTECH, Av. Eduard Maristany 10-14, 08930 Barcelona, Spain
[b] Departament d'Enginyeria Química i Química Analítica, Universitat de Barcelona, Martí i Franquès 1-11, 08028 Barcelona, Spain
[c] Water Technology Center CETaqua, Ctra. d'Esplugues 75, 08940 Cornellà de Llobregat, Spain
[d] EURECAT, Centre Tecnològic de Catalunya, Plaça de la Ciència 2, 08243 Manresa, Barcelona, Spain
[e] Institute of Environmental Assessment and Water Research (IDAEA), Spanish National Research Council (CSIC), c/ Jordi Girona 18-26, 08034 Barcelona, Spain

ARTICLE INFO

Editor: Xiwang Zhang

Keywords:
Water reclamation
Nanofiltration
Solution-electro-diffusion film model
Dissolved organic matter
Fluorescence spectroscopy

ABSTRACT

Nanofiltration (NF) is a promising technology called to play a relevant role in water reclamation, which lies in the core of circular economy in the water sector. The aim of this study was to assess two aromatic polyamide-based NF membranes (the looser NF270 and the tighter NF90 ones) for the treatment of urban impacted phreatic water. The focus was centred on the removal of dissolved inorganic and organic solutes and on the differences observed between solutes. Membrane ions rejection was modelled by the Solution-Electro-Diffusion Film Model (SEDFM). DOC was tracked by Fluorescence Excitation-Emission Matrices (FEEM) coupled to Parallel Factor Analysis (PARAFAC) to get insight into the character of DOC rejected by or permeated through the membranes. Results showed that the NF90 membrane systematically achieved upper values in the rejection of ions than the looser NF270 one. Variations between ions could be interpreted by the mechanisms ruling their rejection, i.e. Donnan and dielectric exclusion phenomena. Experimental rejections were also satisfactorily fit by the SEDFM, indicating that that the presence of DOC in the phreatic water did affect modelling of ions transport through the membranes. DOC was rejected at very high percentages (>90%) by both membranes, but FEEM-PARAFAC analysis revealed that humic- and tryptophan- like components were more rejected (>90% for both membranes) than tyrosine-like compounds (45% for NF270 and 57% for NF90). The finding is of relevance from a point of view of disinfection practices, as it has been observed that humic-like substances are strongly correlated with DBPs formation.

1. Introduction

Growing demands for domestic and industrial uses of water has led to a continuous search for alternative hydric resources not yet exploited, such as poor-quality surface- and ground-water and wastewater. Common constituents of concern in such waters include ions (e.g. NO_3^-, F^-…), metals (e.g. Fe, Mn, Zn, Cd, Cu, Ni…), metalloids (As), Natural Organic Matter (NOM), organic micropollutants (e.g. pesticides, pharmaceutical products and personal care products…) and pathogens, which may pose a serious hazard to all living beings because of their toxicity (of themselves or after reaction with common reagents applied in habitual water treatments) even at low concentrations. Removal of these constituents by an appropriate treatment becomes necessary.

Nanofiltration (NF) is a promising technology that allows to remove most of the above-mentioned constituents from water [1–5]. The unique properties of NF membranes lie between those of Reverse Osmosis (RO) (which uses dense membranes with a very high rejection of almost all dissolved solutes, at expenses of a high operation pressure) and Ultrafiltration (UF) (which uses porous membranes that remove only particulate and colloidal material at a lower operation pressure). Compared to RO and UF, NF offers the advantages of providing high removal of multi-charged ions and NOM, while varying removal ranges for

* Corresponding author.
E-mail address: misael.abenza@upc.edu (M. Abenza).

https://doi.org/10.1016/j.jece.2023.111848
Received 7 February 2023; Received in revised form 22 December 2023; Accepted 29 December 2023
Available online 30 December 2023

single-charged ions and organic micropollutants, together with high water fluxes at relatively low applied pressures and operational costs [6–8].

Understanding the mechanisms behind the rejection of solutes by a NF membrane and the variables that affect them (i.e. active layer composition, pore size and surface charge, water composition, pH, ionic strength, hydrodynamic conditions, interactions solution-membrane…) is complex and remains an ongoing research. The rejection of solutes by NF membranes are acknowledged to be a combination of steric-hindrance (size exclusion) and electrostatic (Donnan exclusion and dielectric exclusion) effects [5,9,10].

The variability of factors and complexity of mechanisms, together with the limited data provided by the manufacturers on the physico-chemical properties of their membranes, make prediction of NF performance difficult. Experimentation still remains the most reliable mean to know the capacity of a NF membrane in removing dissolved solutes. Some models have been developed and refined over the years (e.g. by incorporating phenomena such as the concentration-polarization layer or reactive transport) and can nowadays describe the flux and the retention of solutes by NF membranes quite satisfactorily [11–15]. However, deviations can arise when complex waters are used, e.g. containing various ions and NOM. The latter, which exhibits complexity in structure, character and reactivity, and whose influence on metallic ions rejection predicted by the models is unknown, may add complexity if it interferes with metal rejection [16].

Indeed, understanding NOM behaviour is a current challenge in the water treatment industry. NOM is comprised by a complex and heterogeneous mixture of hundreds compounds that can largely differ in their properties [17]. Although it is known that NOM is generally rejected by NF at high percentages [5,7,8,18,19] it is the NOM character (e.g. aromaticity, hydrophobicity…) that determines the hazards posed by NOM even at the very low concentrations typically found in NF permeates (e.g. formation of disinfection by-products after chlorination of NF permeate) [20]. Advanced techniques for NOM characterisation beyond its quantification as bulk parameters such as Total or Dissolved Organic Carbon (TOC or DOC) have drawn the attention in water treatment research [17].

Three dimensional Fluorescence Excitation-Emission Matrix (FEEM) spectroscopy is one of these techniques for NOM characterisation. Thanks to its high sensitivity, relatively low cost, rapidness of data acquisition at low natural concentrations and potential application as an on-line monitoring tool, FEEM has received increased attention by researchers in the water treatment sector [17,21,22]. However, the interpretation of FEEM spectra may be difficult as they contain a large amount of information on the fluorescence of natural waters, which typically contain a mix of different fluorescent compounds (fluorophores). For this reason, mathematical tools such as peak-picking [23], Fluorescence Regional Integration (FRI) [21] and Parallel Factor analysis (PARAFAC) [24,25] have been developed to decompose overlapping spectra and better analyse the data provided by FEEMs.

To date, numerous investigations on NF have targeted inorganic solutes in synthetic water [26] and in a number of actual source waters, including groundwater [27,28], surface water [7,29] and hydrometallurgical waste streams [30], where NOM was not considered. There are also relatively abundant studies on NOM, usually focusing on its membrane fouling potential, sometimes including FEEM analysis but rarely coupled with PARAFAC [18,19,22,31]. Much fewer are the studies that have evaluated NF membranes for the simultaneous rejection of inorganic solutes and NOM [5,32,33]. In these cases, only few have modelled the rejection of solutes and/or have tracked NOM by FEEM with PARAFAC ([32], focusing on inorganic colloid-NOM mixtures).

The aim of this study was to treat urban phreatic water by NF and evaluate its performance in the simultaneous removal of ions and NOM as analysed by FEEM. Two different aromatic polyamide-based NF membranes were evaluated: Dow Filmtec NF270 and NF90 membranes. The removal of inorganic ions was assessed and modelled by the Solution-Electro-Diffusion Film Model (SEDFM), which takes into account the formation of a concentration-polarization (CP) layer and considers that the transport of solutes through it is due to diffusion, electromigration and convection phenomena. NOM was characterised by FEEM coupled to PARAFAC analysis to identify the nature of NOM that preferentially permeated through the membrane.

2. Materials and methods

2.1. Phreatic water

Phreatic water was collected from a well located approx. 25 m away from the Besòs river in Sant Adrià de Besòs in Barcelona (Spain). The area has been recognised with a high phreatic water level providing huge amounts of water with potential for environmental, municipal and industrial reuse after appropriate treatment [34]. The average composition of the phreatic water is given in Table 1, together with the maximum allowed concentrations set by the EU Directive 2020/2184. As can be seen, Cl^-, Mn and As appeared to be of particularly major concern as they exceeded the legal thresholds (in bold in Table 1). This composition agreed fairly well with that of previous campaigns [34]. Samples were stored in cold conditions without any chemical pre-treatment before being used in our experiments.

2.2. Membranes

Two commercial NF membranes were used in this study: NF270 and NF90 (provided as flat sheet samples by Dow Filmtec). They both are thin-film composite membranes having a three-layered structure comprised of a non-woven polyester, a porous polysulfone supportive layer and an active aromatic/semi-aromatic polyamide layer. The semi-aromatic polyamide layer of the NF270 membrane is fabricated by piperazine (PIP) and trimesoyl chloride, and the fully aromatic polyamide layer of the NF90 membrane by 1,3-benzenediamine and trimesoyl chloride.The polyamide top layer, with a thickness of a few hundred nanometers (<150 nm) but being responsible for the membrane performance, has ionisable carboxylic (RCOOH/R-COO^-) and amine (R-NH_3^+/R-NH_2) groups, that, depending on pH, confer the membrane a positive or negative charge [14]. The ionization behaviour

Table 1
Composition of the phreatic water used in this study and comparison against the European drinking water legislation thresholds. In bold those exceeding the EU directive 2020/2184.

Parameter		Feed water composition	EU Directive 2020/2184
pH		8.0 ± 0.2	6.5 - 9.5
Na	mg/L	167.9 ± 14.6	200
K		17.8 ± 1.5	-
NH_4^+		0.3 ± 0.1	0.5
Mg		48.4 ± 12.7	-
Ca		199.0 ± 28.2	-
Cl^-		**318.0 ± 29.8**	250
NO_3^-		11.8 ± 1.1	50
SO_4^{2-}		131.8 ± 13.6	250
HCO_3^-		438.9 ± 8.8	-
F		< 0.5	-
Br^-		< 0.5	-
HPO_3^{2-}		< 0.5	
B	µg/L	155.5 ± 7.5	1500
Al		36.5 ± 14.4	200
Mn		**139.4 ± 53.9**	50
Ni		5.3 ± 1.6	20
Cu		5.1 ± 0.7	2000
As		**24.2 ± 2.3**	10
Pb		< 1	5
Cd		< 1	5
Cr		< 1	25
Fe		< 1	200
TOC	mg/L	2.3 ± 0.1	Without abnormal changes

of amine groups in polyamide-based NF membranes is described with one pKa (with a value of 3.6), while that of carboxylic groups is described with two pKa (with values in the ranges 5.4–5.7 and 8.7–9.8) depending, among others, on the pore size and the dielectric constant of the microenvironment surrounding them [35]. The main difference between the two membranes is that NF270 is considered "loose" (exhibiting good rejection of high molecular weight NOM and varying rejection of ions while permitting a relatively high flux) whereas the NF90 is considered "tight" (exhibiting high removal of most ions and organic compounds but permitting a low flux).

Membrane manufacturers do not usually offer many details about their membranes beyond the membrane chemistries, the rejection percentage of NaCl and $MgSO_4$ in standardized solutions (e.g. 2 g/L) and molecular weight cut-off (MWCO). In this study, data on the membranes found in the literature were compiled (Table 2). It must be highlighted that there is a lack in uniformity in experimental protocols for the measurement of membrane properties, which are often strongly influenced by operating conditions and system design, making comparison between different studies difficult. Table 2 reports data only from studies that characterised both membranes under the same conditions. Despite disparity in values, all studies concur that looser NF270 membrane is less hydrophobic (with lower contact angle) and more negatively charged (with lower zeta potential) than tighter NF90. NF270 also has a lower surface roughness and thickness of the active layer than NF90. With regard to the effective pore radius shown in Table 2, it must be bear in mind that it represents an imaginary pore radius fitted from experimental results that, in practice, should be viewed only as a guide. Actually, NF and RO dense membranes are considered not to act as an array of cylindrical pores through which solutes molecules pass but to contain intermolecular voids between or interspaces within the polymeric chains of the membrane material through which solute molecules permeate.

2.3. Bench-scale pilot description

The bench-scale filtration system consisted of a thermostated 30-L feed tank (25 ± 2 °C), a flat sheet cross-flow filtration test cell (GE Osmonics SEPA™ CF II) accommodating the membrane coupon (0.014 m^2) and a high pressure diaphragm pump (Hydra-Cell, USA) to pump feed water from the feed tank into the membrane cell. The system was operated in full-recycle mode, i.e. both permeate and retentate were recirculated back into the feed tank (except during sampling), providing thus a fairly constant composition of feed water. The pilot was equipped with required valves (a by-pass valve prior to the test cell and a needle valve placed in the retentate stream) to control transmembrane pressure (TMP) and transmembrane flux. Meters for flow, pressure, conductivity, pH and temperature were also installed for on-line measurements at different locations. A pre-filter cartridge (100 μm, polypropylene) was placed just before the discharge of the retentate to the tank for membrane protection. An arrangement of the lab-scale unit is shown schematically in Fig. 1.

Table 2
Main properties of the NF270 and NF90 membranes.

Parameter	NF270 (loose)	NF90 (tight)
Active layer material	semi-aromatic polyamide	fully aromatic polyamide
Functional groups	Carboxylic acid, amine (secondary)	Carboxylic acid, amine (primary and secondary)
MWCO (Da)	400[a], 155[b], 150–180[c], 150[d]	200[a], 100[b], 120[c], 90[d]
Effective pore radius (nm)	0.36 ± 0.06[c], 0.42[e], 0.35 [f], 0.40 [g]	0.29 ± 0.04[c], 0.34[e], 0.27 [f], 0.31 [g]
Active layer thickness (nm)	14 ± 1 [h]	138 ± 33 [h]
Average roughness (nm)	2.1-4.6[b], 3.68 [f], 5.1 [g], 4 ± 1 [h]	10.8-38.8[b], 27.75 [f], 64.9 [g], 29 ± 6 [h]
Static contact angle (°)	27[b], 18.3 [g], 49 ± 2 [h], 30[i]	54[b], 55.2 [g], 73 ± 2 [h], 63[i]
Isoelectric point (IEP)	3[i]	4[i]
Zeta potential at pH 7 (mV)	-53[g], − 41.03 [h]	-13[g], − 15.19[h]
Effective charge density (mol/m^3)	489[d]	1596[d]
Effective number of pores ($10^6/m^2$)	1.457[j]	1.102[j]
Pure water permeability ($L/m^2 \cdot h \cdot bar$)	10.8[a], 17.5 [g], 27.45 [f]	6.7-8.5[a], 9 [g], 10.16 [f]
$MgSO_4$ rejection (%)(at 4.8 bar)	> 97[a,b]	> 97[a,b]
NaCl rejectionn (%) (at 4.8 bar)	40-60[a], 40-58[c]	85-95[a], 70-90[c]

[a]Manufacturer's data; [b][36]; [c][37]; [d][38]; [e][1]; [f][2]; [g][39]; [h][40]; [i][41]; [j][6]

2.4. Experimental procedure

Prior to any experiment, the virgin membrane coupon was immersed in Milli-Q water for 24 h to remove any preservative product that might be present. Then, the membrane was placed in the cross-flow cell and pressurized for 2 h with distilled water at 32 bar (5 L/min, cross-flow velocity of 1 m/s) for 90 min and at 22 bar for 30 min. Next, the membrane was compacted for 2 additional hours with feed solution (phreatic water from the Besòs aquifer) under the same conditions before the start of an experiment. Once an experiment started, the membrane was characterised in terms of hydraulic permeability and ion and dissolved organic carbon (DOC) rejection. For this purpose, the TMP was gradually varied from 5 bar to 32 bar while maintaining constant the cross-flow velocity at 0.7 m/s (3.46 mL/min). As stated above each experiment was carried out under full recirculation of both retentate and permeate. Samples of permeate were collected at each TMP tested after stabilization of the system, which was ascertained from constant flux and conductivity value in the permeate. On the completion of the experiment, feed water was exchanged with distilled water, which was used to clean the membrane and the whole system at a 5 L/min at 10 bar (for 30 min) and at 22 bar (for 90 min). All experiments were done in duplicate.

2.5. Water sampling and analysis

2.5.1. Bulk parameters and inorganic ions

A follow-up of the permeate flow rate and composition was carried out throughout the experiments. The flow rate was measured by weighing permeate volumes for a given period of time. During the experiment, electrical conductivity and pH were measured by means of an EC-Metro GLP31 and a GLP22, respectively (both provided by Crison). Major and minor ions were analysed after filtration (0.22 μm) by several techniques. Hydrogencarbonate (HCO_3^-) was analysed by titration using an autotitrator model T70/Rondolino controlled with LabX titration software and HCl as titrator. Major ions (in the range of mg/L) were analysed by ionic chromatography (IC) (Dionex, ICS-1000, Thermo-Fisher Scientific, USA) coupled to cationic and anionic detectors (ICS-1000 and ICS-1100, respectively) and controlled by the chromatographic software Chromeleon®. Columns CS16 (4 ×250 mm) and AS23 (4 ×250 mm) (Phenomenex, Barcelona, Spain) were used for cation and anion determination, respectively. Minor ions (in the range of μg/L) were analysed by inductively coupled plasma optical emission spectrometry (ICP-OES, Agilent, 5100 ICP-OES) and mass spectrometry (ICP-MS, Agilent, 7800 ICP-MS) after filtration (0.22 μm) and acidification of the samples (2% HNO_3). DOC in filtered (0.45 μm) samples was quantified using a TOC analyser (Shimadzu TOC-V CPH) by measuring the difference between the total carbon and inorganic carbon (acidification with 2 M HCl). Analytical precision and accuracy were tested against Reference Material provided by the DOC-CRM program (University of Miami-D.A. Hansell). The quality assurance/quality control (QA/QC) protocol comprised the calibration of the instruments with five

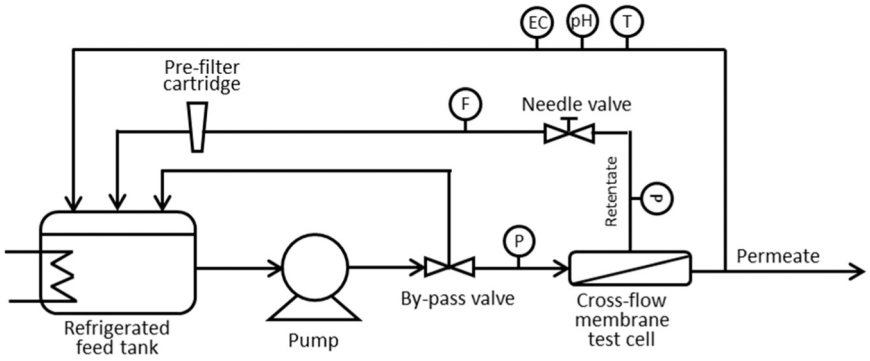

Fig. 1. Scheme of the cross-flow filtration experimental set-up used in this study. In-line monitoring sensors and auxiliary components are also shown (P: pressure, F: flow, EC: electrical conductivity).

standards covering the range of the experimental concentrations before each use. Furthermore, one blank and one duplicate sample were analysed after every 15 experimental samples.

2.5.2. FEEM-PARAFAC analysis

FEEM spectra were collected on an Agilent Cary Eclipse fluorescence spectrophotometer, controlled by Cary Eclipse Scan Application version 1.2, using a PC running the Microsoft Windows 7 operating system. Fluorescence intensities were measured using a 1 cm path length Hellma QS quartz cuvette at excitation wavelengths (λ_{ex}) of 225–400 nm and emission wavelengths (λ_{em}) of 250–500 nm, both in 5 nm increments, using a scan speed of 600 nm/min. The slit widths on excitation and emission modes were both set at 5 nm. The photomultiplier tube voltage was set to 600 V. MilliQ water was run as blank and its FEEM spectrum was subtracted from the sample one in order to reduce the influence of Raman scattering. The processed FEEM spectra were then plotted using Origin Lab.

Decomposition of the FEEM spectra into their underlying chemical components was accomplished by PARAFAC analysis. Data treatment was performed using the DOMfluor Toolbox [24] and N-way Toolbox [42] under the MATLAB environment (The MathWorks, Inc., Natick, LEVEL, USA). The number of fluorescence components was determined by examination of residual errors. Component spectra were also compared against the on-line repository of published fluorescence spectra OpenFluor (www.openfluor.org) to evaluate spectral matching and component identification [25].

2.6. Mas transport model for description of ions rejection by NF membranes

For each experiment the rejections of major and minor inorganic solutes versus transmembrane flux were fitted with the Solution-Electro-Diffusion Film Model (SEDFM). This model takes into account the formation of a concentration-polarization (CP) layer and considers that the transport of a solute through the CP layer is due to diffusion, electro-migration and convection while its transport through the membrane (which has no pores but a free-volume where no convective flux occurs) is due to diffusion and electromigration. The fluxes can be described by the following equations [11]:

$$\text{Flux through the CP layer}: \; J_i = -P_i^{\delta}\cdot\left(\frac{dc_i^{'}}{dx^{'}} - z_i c_i^{'}\frac{d\varphi^{'}}{dx^{'}}\right) + J_v c_i^{'} \qquad (1)$$

$$\text{Flux through the membrane}: \quad J_i = -P_i\cdot\left(\frac{dc_i}{dx} - z_i c_i\frac{d\varphi}{dx}\right) \qquad (2)$$

where J_i and J_v are the molar transmembrane fluxes of solute i and solvent (μmol/(m^2·s) and μm/s, respectively), respectively, P_i^{δ} and P_i are the permeances to solute i of the CP layer and the membrane, respectively, (μm/s), $c_i^{'}$ and c_i are the concentrations of solute i in the CP layer and membrane, respectively (mol/m^3), x′ and x are the normalized positions in the CP layer and membrane, respectively (from 0 to 1) (−), z_i is the charge of solute i, and $\varphi^{'}$ and $\varphi$are the dimensionless electrostatic potentials within the CP layer and membrane, respectively (−). The terms on the right-hand side of Eq. 1 represent the transport of the solute due to diffusion, electro-migration and convection, respectively. A deeper description of the model and the protocol of data treatment for the SEDFM has been reported in previous works [15,43,44].

3. Results and discussion

3.1. Solutes rejection by NF membranes as a function of trans membrane flux

Fig. 2 shows the dependence of permeate flux on transmembrane pressure (TMP) during the filtration experiments. For both membranes the permeate flux at steady-state increased, as expected, with the applied TMP following a linear relationship according to the well-known equation of water transport through membranes. Also as expected, and in accordance with published works [2,26,27], the looser NF270 membrane displayed a slightly greater average value of permeability (2.50 μm/s·bar) than the tighter NF90 membrane (1.73 μm/s·bar).

Fig. 3 shows the rejection of major and minor inorganic solutes versus transmembrane flux for membranes NF270 (Figs. 3a and 3b) and NF90 (Figs. 3c and 3d). Rejections from duplicates experiments differed by less than 5%. The figure also plots the fitting of these experimental values with the SEDFM model (continuous lines).

Two general observations can be drawn from Fig. 3. First, rejection for all solutes was clearly lower (or equal) for the looser NF270 membrane than for the tighter NF90 membrane, in agreement with published studies comparing the NF270 and NF90 membranes [2,6]. The reason of

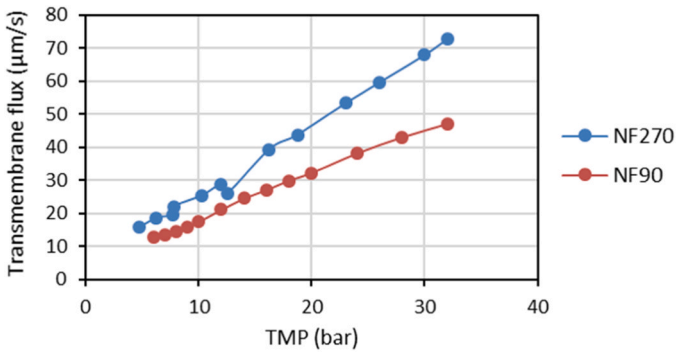

Fig. 2. Permeate flux dependence on transmembrane pressure during the filtration experiments.

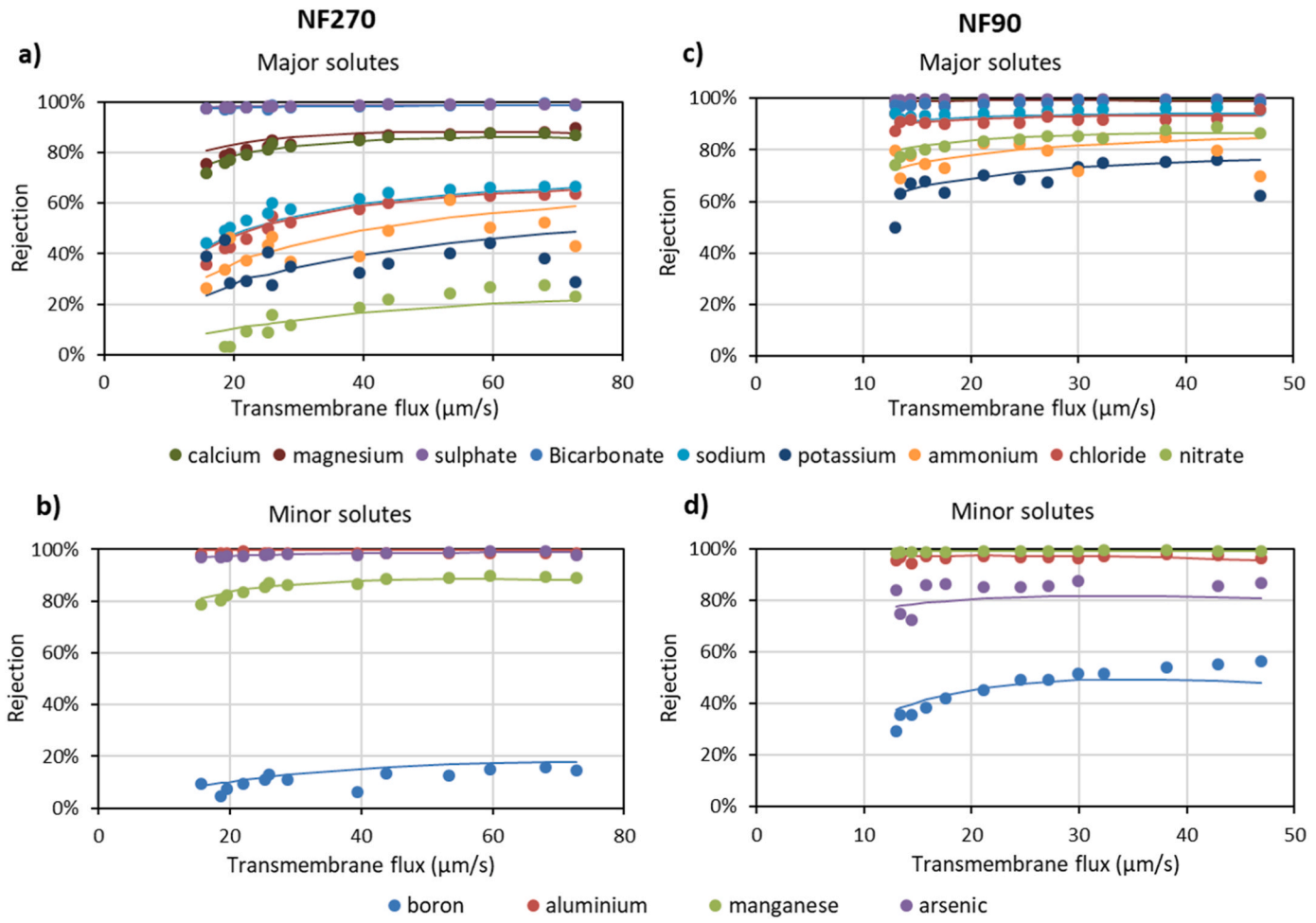

Fig. 3. Variation of major and minor inorganic solutes removal versus transmembrane flux for membrane NF270 (a and b) and NF90 (c and d). Full lines correspond to the fitting of experimental values (points) with the SEDFM.

the higher rejection values by the NF90 membrane lies in its minor effective radius pore, which intensifies the mechanisms governing the solutes' rejection (described below). Second, regardless of the membrane used, rejection for a given solute increased with transmembrane flux, indicating that at higher TMPs the CP was partially mitigated by shear forces, with the subsequent decrease of solute concentration on the vicinity of the membrane and of solute permeation. Moreover, at higher TMPs, the increase in permeation of water (while that of ions remaining unchanged as it happens with dense membranes with no coupling between transport of solute and water) diluted the solute concentration in the permeate side and increased the observed solute rejection [37].

Beyond these general trends, further considerations must be made to explain variations observed between solutes, particularly with regards to the electrostatic interactions between charged solutes (i.e. ions) and the membrane. The transport of an ion through a charged membrane is governed by two exclusion mechanisms: the Donnan and the dielectric phenomena. The first postulates that co-ions (the ions having the same sign of charge as that of the membrane surface) are repelled by the membrane (resulting in a higher rejection), while counter-ions are attracted by the membrane (resulting in an easier approach to and permeation through the membrane). However, the gradient of concentrations between the bulk phase (with higher concentration of co-ions) and the membrane (with higher concentration of counter-ions) creates a potential difference (the Donnan potential) that prevents counter-ions from passing the membrane in order to maintain electroneutrality on the feed side of the membrane [5,12]). Nevertheless, the Donnan exclusion mechanism alone cannot explain the differences in rejections between single- and multi-charged ions. The second phenomenon stems from the resistance of a hydrated ion to penetrate the membrane (which has a dielectric constant different from that of water) due to the hydration shell. As the energy required for the shedding of the hydration shell is proportional to the square of the ion charge (and independent of the charge sign) double-charged solutes (irrespective of the charge sign) are more rejected than single-charged solutes [12,14]. Whatever the electrostatic phenomena taking place, electroneutrality must be achieved in both sides of the membranes, so that the passage of most mobile ions (i.e. with lowest charge and size) through the membrane will be preferential. With regard to neutral species, they are not affected by the membrane charge and their rejection is ruled only by size-exclusion phenomenon.

For all this, charges of membranes and solutes must be identified. In this study, pH of feed water (8.1) was higher than IEP of both NF270 and NF90 membranes (3.0–4.0, see Table 2), and therefore they were expected to have their functional groups amine and carboxylic groups deprotonated ($R–NH_3$ and $R–COO^-$, respectively) and, thus, exhibit a negative charge on their surface. With regard to the charges of solutes, it must be bear in mind that not all of them were necessarily found as free ions. Table 3 gives the speciation for each solute considering the matrix of the water treated using the software packages Hydra and Medusa [45]. For elements with more than one species, the table shows the prevalence percentage and the charge for each species. Fig. 4 shows the speciation diagram for sulphate as an example. As seen in Table 3, although free ions were the prevalent species for all elements (e.g. Ca^{2+},

Table 3
Predicted speciation for each solute in feed water, showing the prevalence percentage and the charge for each species. Percentages should be viewed as an estimation, as calculations used with the numerical code Hydra and Medusa [45] are based on assuming chemical equilibrium conditions.

Major solutes			Minor solutes		
	Species	Charge		Species	Charge
Calcium	Ca^{2+}: 85%	+ 2	Boron	H_3BO_3: 100%	0
	$CaSO_4$(aq): 11%	0	Aluminium	*	
	$CaHCO_3^+$: 4%	+ 1	Manganese	Mn^{2+}: 67%	+ 2
Magnesium	Mg^{2+}: 84%	+ 2		$MnHCO_3^+$: 17%	+ 1
	$MgSO_4$(aq): 12%	0		$MnSO_4$(aq): 9%	0
	$MgHCO_3^+$: 4%	+ 1		$MnCO_3$(aq): 7%	0
Sulphate	SO_4^{2-}: 43%	-2	Arsenic	$HAsO_4^{2-}$: 95%	-2
	$CaSO_4$(aq): 35%	0		$H_2AsO_4^-$: 5%	-1
	$MgSO_4$(aq): 20%	0			
	$NaSO_4^-$: 2%	-1			
Bicarbonate	HCO_3^-: 92%;	-1			
	$CaHCO_3^+$: 3%	+ 1			
	H_2CO_3 (as CO_2): 2%	0			
	CO_3^{2-}: 3%	-2			
	$MgHCO_3^+$: 1%	+ 1			
Sodium	Na^+: 100%	+ 1			
Potassium	K^+: 100%	+ 1			
Ammonium	NH_4^+: 95%	+ 1			
	NH_3: 5%				
Chloride	Cl^-: 100%	-1			
Nitrate	NO_3^-: 100%	-1			

* Aluminium can be found in multiple forms including mononuclear species (e.g. $Al(OH)^{2+}$, $Al(OH)_2^+$, $Al(OH)_3$(aq), $Al(OH)_4^-$.), polymerised forms ($[Al_2(OH)_2]^{4+}$, $[Al_6(OH)_{12}]^{6+}$…), ion complexes with co-existing anions ($AlSO_4^+$.) or complexes with organic ligands.

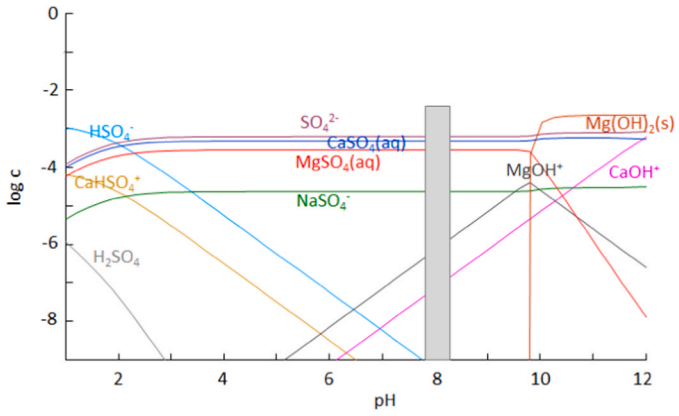

Fig. 4. Species distribution diagram (built using Hydra Medusa [45]) as a function of pH for sulphate in phreatic water from Sant Adrià de Besòs used in the experiments. The concentration of each species is expressed on a logarithmic scale. The grey bar indicates the pH range of the phreatic water.

Mg^{2+}, SO_4^{2-}, Na^+, Cl^-, Mn^{2+}…), uncharged or charged ion complexes (e.g. $CaSO_4$(aq), $MgHCO_3^+$, $MnHCO_3^+$…) could also be present.

As seen in Fig. 3, double-charged ions (such as SO_4^{2-}, $HAsO_4^{2-}$, Ca^{2+}, Mg^{2+} and Mn^{2+}) were the most rejected ions by both membranes (with rejection percentages between 73–99% for the looser NF270 and >95% for the tighter NF90 membrane), in accordance with the dielectric exclusion phenomenon. Differences between these ions can be explained by the Donnan exclusion phenomenon: negatively charged sulphate and arsenic oxyanion (found mostly as double-charged species SO_4^{2-} and $HAsO_4^{2-}$ with contributions of single-charged and/or neutral species as shown in Table 3) were more repelled by the negatively charged membrane and therefore more rejected than positively charged calcium and magnesium (found mostly as double-charged free ions Ca^{2+} and Mg^{2+} with moderate percentages of as single-charged $CaHCO_3^+$ and $MgHCO_3^+$). The unexpected lower As rejection for the tighter NF90 membrane can be related to the higher acidification observed for this membrane (see sub-Section 3.2 below), with a pH observed in the permeate of 6.8, lower than the observe done in the NF270-permeate (7.7). Considering that pKa_2 of H_3AsO_4 is 7.0, it was expected that As was found as single-charged species $H_2AsO_4^-$ at a higher percentage for the NF90 membrane (54%) than for the NF270 membrane (16%) and consequently less rejected.

On the other hand, single-charged ions clearly showed lower rejections than double-charged ones (below 66% for the looser NF270 and between 50–95% for the tighter NF90). These included cations (K^+, NH_4^+, Na^+ and H^+) and anions (NO_3^- and Cl^-). Despite the Donnan mechanism, anions permeated through the membrane (particularly NO_3^-) to ensure electroneutrality at both sides of the membrane. Protons H^+, although being at a very low concentration in comparison to the other ions, deserve a discussion apart, as done below.

It is worth noting that HCO_3^-, despite being a single-charged ion, showed a remarkably high rejection (>90%). These high values can be due to a likely calcite scaling on the membranes. Similar high HCO_3^- rejections have been observed by López et al. [15] and Owusu-Agyeman et al. [46].

Finally, boron, the only monitored element found entirely in an uncharged form (H_3BO_3, pKa=9.25 at 298 K) at the neutral pH of the feed water, exhibited the lowest rejection among the dissolved species (below 20% for looser the looser NF270 and between 25–59% for the tighter NF90). The neutral character of H_3BO_3, together with its small size (its radius has been estimated to be 0.155 nm [47] relative to the pore radius of the membrane (Table 2), explains the low rejection over the whole TMP range tested, which took place solely by size exclusion. Similar low rejection for B at neutral pH by polyamide-based NF membranes can be found in the literature [48].

The rejection percentages observed in this study were consistent with published works reporting the superiority of the NF90 membrane over the NF270 membrane, with the former showing high rejections (>90%) for multi-charged ions but high-to-moderate (50–90%) for single-charged species, and the latter showing similar high rejections (>90%) for multi-charged species but something lower (50–70%) for positively charged calcium and magnesium and moderate-to-low (30–60%) for single-charged species (but much lower for chloride and nitrate) [7,26–29]. When included as monitored species, B was seen to be hardly rejected (<30% for NF90 and <10% for NF270) similarly to our study. Slight discrepancies in rejection percentages between studies may come from differences in waters treated, which included

groundwater [27,28], surface water [7,29] or synthetic water [26] whose matrices naturally affected the speciation of solutes but also the properties of the membranes. For instance, Ca^{2+} and Mg^{2+} have been found to bind to carboxylic and amine groups of the membrane material, weakening ions rejection by charge exclusion [5,10]. On the other hand, NOM can form metal-NOM complexes altering the behaviour of metal ions [16]. The Ca, Mg and TOC contents in the aforementioned studies ranged from 0 mg/L [26] to, respectively, 280 mg/L, 240 mg/L and 8 mg/L [29], comprising intermediate values [7,27,28].

3.2. Bicarbonate ions permeation and permeate pH

Worth mentioning was the effect of the different HCO_3^- rejection by NF270 and NF90 membranes on permeate pH. When negatively-charged HCO_3^- (and also the small amounts of CO_3^{2-} present at feed pH of 8.1) was rejected (but not neutral H_2CO_3), the equilibrium with H_2CO_3 got disrupted in the permeate side. In order to recover the equilibrium, H_2CO_3 dissociated providing HCO_3^- and H^+ and decreasing pH in the permeate. In other words, higher rejections of HCO_3^- were expected to be accompanied by lower permeate pHs. This was in consonance with what was observed in the experiments: the higher removal of HCO_3^- by the NF90 membrane was accompanied by an acidification of the permeate (in comparison with the NF270) (Fig. 5).

A second effect can contribute to the acidification in the permeate side: the high rejection of cations (by the negatively charged membrane) through the Donnan mechanism and the need to keep electroneutrality in the permeate side made cations with highest mobility be forced to permeate (preferentially over other cations with lower mobility). Among cations, the most mobile one was H^+, resulting in a decrease of pH in the permeate. This effect was more evident in the case of the tighter NF90 membrane, where higher rejection of cations were attained, with the subsequent lower pH in the permeate. Similar acidification of NF permeates due to H^+ permeation have been reported [15, 38].

3.3. Modelling of observed rejections with SEDFM

The experimentally obtained solute rejections were fitted by the SEDFM, whose predictions are represented with full lines in Fig. 3. As can be seen, the SEDFM model showed good fit with the experimental data, pointing out that the assumptions of the SEDFM were correct and that the presence of organic matter in the phreatic water did not seem to affect modelling of transport of inorganic species through the membrane. This was probably because the level of TOC in the phreatic water in Sant Adrià de Besòs was low (2.3 mg/L). Haddad et al. [5] observed that the presence of NOM at concentrations $\leq$ 1 mg/L did not affect the rejection of Mn and Fe, and attributed this marginal influence to the low levels of NOM and the subsequent low formation of NOM complexes with Fe.

Table 4 shows the permeance values provided by the model for all

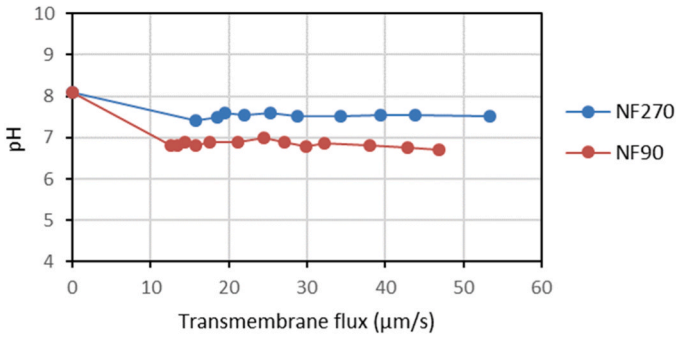

Fig. 5. Changes in permeate pH vs transmembrane flux for membranes NF270 and NF90.

Table 4
Permeance values for inorganic solutes through NF270 and NF90 membranes provided by the SEDFM.

	Membrane permeances to solutes, P_i (µm/s)	
	NF270	NF90
Calcium	4.6	0.1
Magnesium	3.2	0.1
Sulphate	0.2	< 0.1
Bicarbonate	0.3	0.2
Sodium	22.7	1.3
Potassium	78.3	12.2
Ammonium	45.2	6.4
Chloride	14.9	0.8
Nitrate	67.9	1.9
Boron	68.7	8.0
Aluminium	0.1	0.4
Manganese	3.1	0.1
Arsenic	0.5	44.7

solutes. The order of permeance values were in general agreement with the rejections observed. For instance, permeances for well rejected double-charged ions were all < 5 µm/s for NF270 and < 0.5 µm/s for NF90, while permeances for generally poorly rejected single-ions were mostly ≥ 15 µm/s for NF270 and ≥ 1 µm/s for NF90. For the neutral B species, permeance value was approx. 69 µm/s for NF270 and 8 µm/s for NF90. Moreover, the values obtained supported the fact that both membranes presented a negative charge at the operating conditions. As example, the membrane permeances to anions were lower than the ones for cations, in agreement with Donnan exclusion. For example, the membrane permeance to Cl^- was 14.93 and 0.84 µm/s for NF270 and NF90, respectively, while the values to Na^+ were 22.73 and 1.28 µm/s. Moreover, the effect of dielectric exclusion can be observed as membrane permeances to multi-charged elements were always lower than the one for mono-charged ones. As example, permeances to SO_4^{2-} were up to 2 orders of magnitude than the ones for Cl^-, having values of 0.23 and 0.02 µm/s for NF270 and NF90, respectively.

3.4. DOC rejection by NF membranes and quantification by FEEM

As expected and in agreement with published studies with NF270 and NF90 [5,7,8,18,19], DOC was rejected at very high percentages (>90%) by both membranes. Retention of NOM by these polymeric membranes was attributed to both size effects (as most NOM compounds are >1000 Da in size and thus sieved by the NF membranes) and charge effects (as most NOM compounds are negatively charged at neutral pHs and thus repelled by the negatively charged NF membranes) [7].

However, the relevance of residual DOC in permeate lies not only in its concentration but also in its character. The FEEM spectra of feed water and a representative NF permeate for both NF270 and NF90 membranes are depicted in Fig. 6. The spectra are divided into five regions according to the operational definition given by Chen et al. [21], in which region I-II corresponds to aromatic protein-like material, region III to fulvic acid-like material, region IV to microbial by-product-like material and region V to humic acid-like material.

Fluorescence of feed water was clearly dominated by region III (fulvic acid-like fluorophores), whereas contribution of fluorophores in regions I-II, IV and V were weaker (Fig. 6a and c). Permeate FEEM spectra reflected substantial reduction in intensity of fulvic acid- and humic acid-like materials (regions III and V), whereas signal of protein-like (region I-II) and soluble microbial by-product-like (region IV) remained more unchanged (Fig. 6b and d), suggesting that these latter fluorophores better permeated through both NF membranes.

In this study, PARAFAC analysis was applied to FEEM spectra to get further insight into the fluorescent substances. A 6-components model best fitted the FEEMs obtained and therefore it was the one considered for further analysis. Fig. 7 plots the excitation and emission spectra of each of the six components. The excitation loadings exhibited two

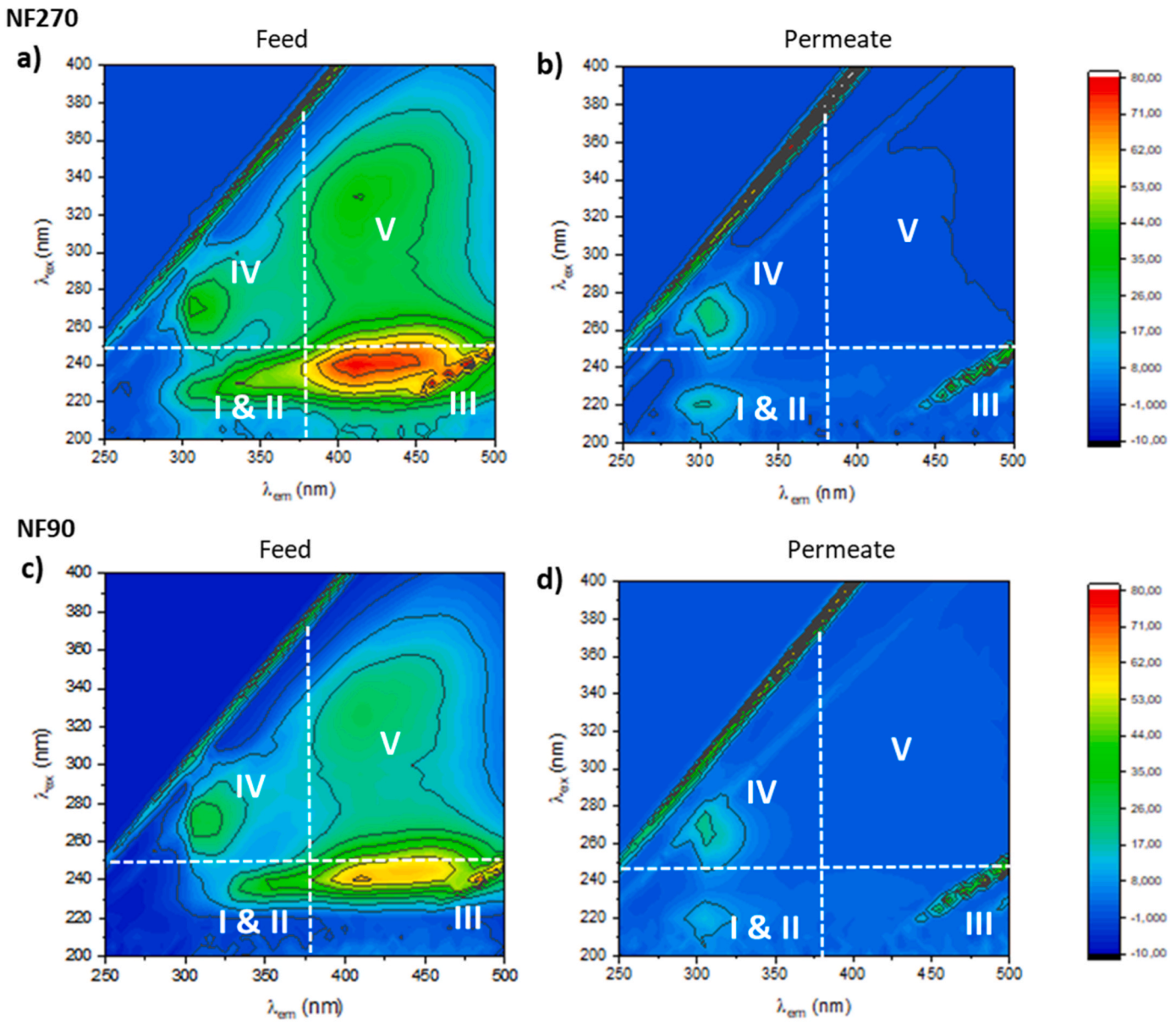

Fig. 6. FEEM contours of feed water and permeate for NF270 membrane (a and b, respectively) and NF90 membrane (c and d, respectively).

maxima whereas the emission loadings a single maximum for almost all components.

All six components (C1-C6) have been reported in the literature of DOC fluorescence (and mostly match other works with a minimum similarity score of 0.95 in the database Openfluor). Components C1, C2 and C3 are associated to humic-like substances, C4 to protein-like tryptophan-containing substances, and C5 and C6 to protein-like tyrosine-containing substances [17,19,22,49].

The maximum fluorescence intensity (F_{max}) of each component was used to represent its relative concentration. Fig. 8 shows F_{max} signals of the six components for feed water and three permeate samples (corresponding to three different operation pressures) for both NF270 (Fig. 8a) and NF90 (Fig. 8b) membranes. Feed water exhibited higher F_{max} for C1 and C2, whereas F_{max} for C4 and C6 were much lower. Surprisingly, feed water for NF90 did not show any fluorescence for C5 and that of C3 was much lower in comparison to feed for NF270. The reason behind this might be fluctuations in composition of groundwater during the sampling campaign.

For both NF membranes the greatest reductions in F_{max} was observed for C1, C2, C3 and C4, with reduction percentages generally > 90% (for both NF270 and NF90 membranes), as opposite to C6, whose peak was reduced at average percentages of only 45% for NF270 and 57% for NF90. When present in feed water for NF270, peak for C5 was reduced by even a lower percentage (20%). Interestingly, these results highlighted differences in rejection among types or fluorescent organic substances: while components C1-C4 (humic- and tryptophan-like compounds) were successfully rejected, components C5 and C6 (tyrosine-like compounds) were not. The TMP did not seem to exert any remarkable effect on the reduction of F_{max} for any component, at least in the range 7.7–59.6 bar.

The reason of this diversity in rejection between components may lie in the differences in their molecular sizes and hydrophobicity. In fact, it has been reported that "DOM fluorescence shown at longer λ_{em} could be associated with larger sized molecules and a more hydrophobic nature" [22]. C5 and C6 showed the shortest λ_{em} (Fig. 7) and likely showed the lowest size, explaining thus its lower rejection in comparison with C1-C4, which showed longer λ_{em} (Fig. 7). This finding agrees with that of Li et al. [19], who observed that NF could almost entirely remove all components excepting that corresponding to tyrosine-like compounds. The finding is also in line with other works focused on the fouling

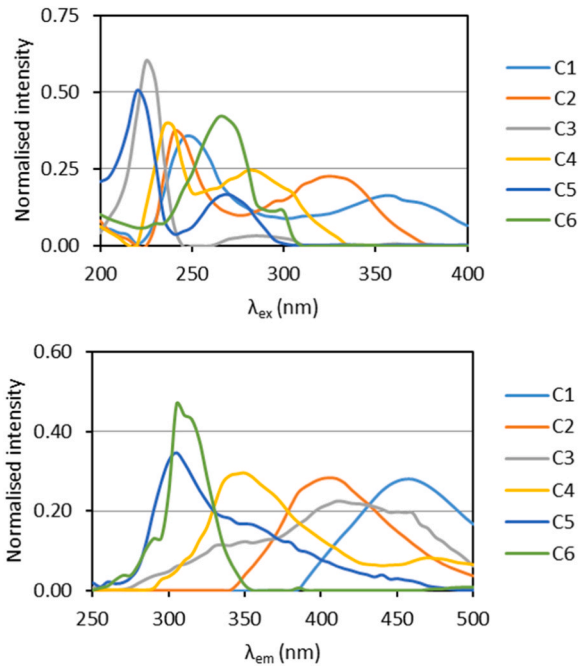

Fig. 7. Loadings plots of components C1-C6 identified by PARAFAC analysis in the assumption of 6-model components.

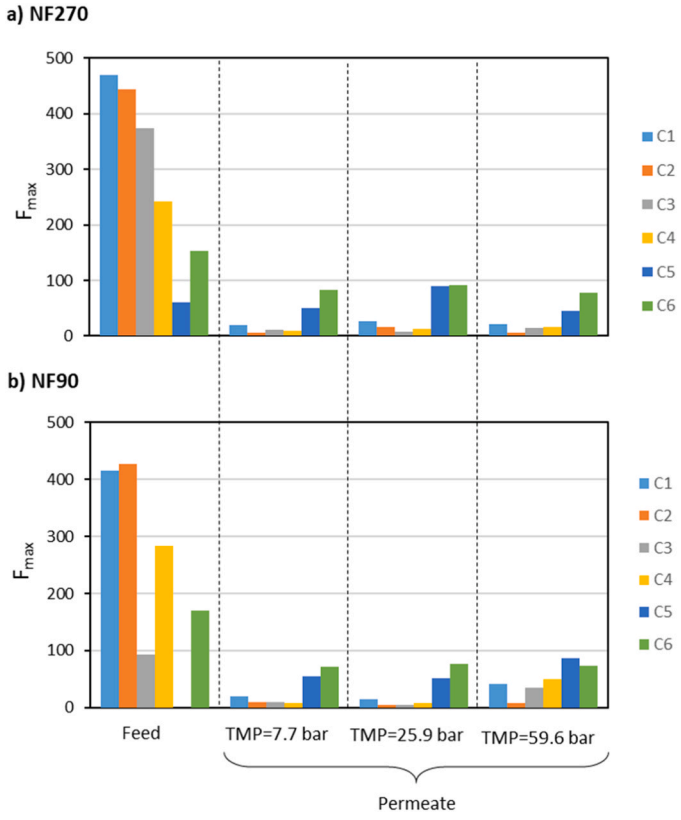

Fig. 8. Reductions in maximum fluorescence intensity (Fmax) for components C1-C6 by a) NF270 and b) NF90 membranes as a function of the transmembrane pressure (TMP).

potential of NOM fractions tracked by FEEM that report that tyrosine-like was associated with lower molecular weight molecules and, as such, represented a key foulant in NF membranes in opposition to larger molecular weight molecules [22,31,49]. The finding would also be in concordance with Meylan et al. [3] and Owusu-Agyeman et al. [46], who concluded that the small fraction of DOC that permeated their NF membranes was mostly composed of neutral low molecular weight compounds. The finding that humic-like substances were preferentially rejected by NF is of relevance from a point of view of disinfection practices, as it has been observed that humic-like substances are strongly correlated with DBPs formation [50]).

4. Conclusions

Two different polyamide NF membranes (the Dow Filmtec looser semi-aromatic NF270 and the tighter fully aromatic NF90) were evaluated for the treatment of phreatic water. Results showed that these membranes performed differently: overall, the tighter membrane (NF90) resulted in higher rejections of ions, at expenses of a lower flux, than the looser membrane (NF270). In accordance with the Donnan and dielectric exclusion mechanisms, double-charged ions were more rejected (with rejection percentages >95% for the NF90 membranes and between 73–99% for the NF270 membrane) than single-charged ions (between 50–95% for the NF90 membrane and <66% for the NF270 membrane), and anions were generally more rejected than cations by both negatively-charged NF90 and NF270 membranes. In order to keep electroneutrality in the permeate side, H^+ showed an enhanced permeability, with the subsequent acidification of the permeate. This decrease in pH was more evident for the NF90 membrane, as rejection of ions was higher. The SEDFM proved to satisfactorily fit the experimental results, pointing out that the assumptions of the model were correct and that the presence of organic matter in the phreatic water did not affect modelling of ion transport through the NF membranes. Dissolved organic carbon (DOC) was rejected at very high percentages (>90%) by both membranes, but revealing differences between fractions as analysed by FEEM: while humic- and tryptophan- like components were highly rejected (at percentages generally >90% for both NF270 and NF90 membranes), tyrosine-like compounds were rejected at comparatively lower percentages (45% for NF270 and 57% for NF90). The finding is of relevance from a point of view of disinfection practices, as it has been observed that humic-like substances are strongly correlated with DBPs formation. The capacity of distinguishing behaviours of different organic fractions provides FEEM+PARAFAC a great potential in fast tracking NOM in treatment water processes. From a point of view of the possible uses of treated water, it must be stated that, despite the differences in solutes rejection percentages, the permeates obtained from both membranes exhibited high quality, with all analysed parameters below the threshold set by the EU Directive 2020/2184 for drinking water and by the Spanish RD 1620/2007. This highlighted that phreatic water from the aquifer of Sant Adrià de Besòs has potential for safe potable water production if adequately treated by nanofiltration.

CRediT authorship contribution statement

Gibert Agulló Oriol: Conceptualization, Investigation, Project administration, Supervision, Validation, Writing – review & editing. **Vázquez-Suñé Enric:** Investigation, Supervision, Writing – review & editing. **de Pablo Joan:** Project administration, Resources, Supervision, Writing – review & editing. **Cortina José Luis:** Conceptualization, Investigation, Supervision, Writing – review & editing. **Beltrán José Luis:** Data curation, Methodology, Supervision, Writing – review & editing. **López Julio:** Data curation, Formal analysis. **Abenza Martínez Misael:** Investigation, Methodology, Writing – original draft, Data curation.

Declaration of Competing Interest

Hereby, the authors declare that the content of this article is subject to no conflict of interest.

Data Availability

Data will be made available on request.

Acknowledgements

This study received funding from the PECT Litoral Besòs: Territori Sostenible project, partially funded by the European Regional Development Fund (FEDER) (GO03-003358), and the R2MIT project (CTM2017–85346-R) and W4V (PID2020-114401RB-C21) projects, funded by the Research Spanish Agency (AEI) Spanish Ministry of Economy and Competitiveness (MINECO). Financial support was also received from the Catalan AGAUR Agency through the Research Groups Support program (2021-SGR-GRC-00596). Authors also thank J. Nadal for his laboratory assistance, M. Fernández for the ICP-MS measurements and Dow-Dupont for NF270 and NF90 for membranes supply. Additionally, the authors acknowledge the OpenInnovation – Research Translation and Applied Knowledge Exchange in Practice through University-Industry-Cooperation (OpenInnoTrain), Grant agreement number (GAN): 823971, H2020-MSCA-RISE-2018–823971.

References

[1] L.D. Nghiem, A.I. Schäfer, M. Elimelech, Removal of natural hormones by nanofiltration membranes: measurement, modeling and mechanisms, Environ. Sci. Technol. 38 (2004) 1888–1896, https://doi.org/10.1021/es034952r.
[2] N. Hilal, H. Al-Zoubi, A.W. Mohammad, N.A. Darwish, Nanofiltration of highly concentrated salt solutions up to seawater salinity, Desalination 184 (2005) 315–326, https://doi.org/10.1016/j.desal.2005.02.062.
[3] S. Meylan, F. Hammes, J. Traber, E. Salhi, U. von Gunten, W. Pronk, Permeability of low molecular weight organics through nanofiltration membranes, Water Res 41 (2007) 3968–3976, https://doi.org/10.1016/j.watres.2007.05.031.
[4] C.L. Patterson, A. Anderson, R. Sinha, N. Muhammad, D. Pearson, Nanofiltration membranes for removal of color and pathogens in small public drinking water sources, J. Environ. Eng. 138 (2012) 48–57, https://doi.org/10.1061/(ASCE)EE.1943-7870.0000463.
[5] M. Haddad, T. Ohkame, P.R. Bérubé, B. Barbeau, Performance of thin-film composite hollow fiber nanofiltration for the removal of dissolved Mn, Fe and NOM from domestic groundwater supplies, Water Res 145 (2018) 408–417, https://doi.org/10.1016/j.watres.2018.08.032.
[6] K. Košutić, D. Dolar, B. Kunst, On experimental parameters characterizing the reverse osmosis and nanofiltration membranes' active layer, J. Membr. Sci. 282 (2006) 109–114, https://doi.org/10.1016/j.memsci.2006.05.010.
[7] Á. de la Rubia, M. Rodríguez, V.M. León, D. Prats, Removal of natural organic matter and THM formation potential by ultra- and nanofiltration of surface water, Water Res 42 (2008) 714–722, https://doi.org/10.1016/j.watres.2007.07.049.
[8] A. Lidén, K.M. Persson, Comparison between ultrafiltration and nanofiltration hollow-fiber membranes for removal of natural organic matter: a pilot study, J. Water Supply Res. Trans. 65 (2016) 43–53, https://doi.org/10.2166/aqua.2015.065.
[9] C. Bellona, J.E. Drewes, P. Xu, G. Amy, Factors affecting the rejection of organic solutes during NF/RO treatment—a literature review, Water Res. 38 (2004) 2795–2809, https://doi.org/10.1016/j.watres.2004.03.034.
[10] M.R. Teixeira, M.J. Rosa, The impact of the water background inorganic matrix on the natural organic matter removal by nanofiltration, J. Membr. Sci. 279 (2006) 513–520, https://doi.org/10.1016/j.memsci.2005.12.045.
[11] A. Yaroshchuk, M.L. Bruening, E.E. Licón Bernal, Solution-diffusion-electro-migration model and its uses for analysis of nanofiltration, pressure-retarded osmosis and forward osmosis in multi-ionic solutions, J. Membr. Sci. 447 (2013) 463–476, https://doi.org/10.1016/j.memsci.2013.07.047.
[12] A.W. Mohammad, Y.H. Teow, W.L. Ang, Y.T. Chung, D.L. Oatley-Radcliffe, N. Hilal, Nanofiltration membranes review: recent advances and future prospects, Desalination 356 (2015) 226–254, https://doi.org/10.1016/j.desal.2014.10.043.
[13] O. Agboola, J. Maree, A. Kolesnikov, R. Mbaya, R. Sadiku, Theoretical performance of nanofiltration membranes for wastewater treatment, Environ. Chem. Lett. 13 (2015) 37–47, https://doi.org/10.1007/s10311-014-0486-y.
[14] J. López, M. Reig, A. Yaroshchuk, E. Licon, O. Gibert, J.L. Cortina, Experimental and theoretical study of nanofiltration of weak electrolytes: $SO_4^{2-}/HSO_4^-/H^+$ system, J. Membr. Sci. 550 (2018) 389–398, https://doi.org/10.1016/j.memsci.2018.01.002.
[15] J. López, A. Yaroshchuk, M. Reig, O. Gibert, J.L. Cortina, An engineering model for solute transport in semi-aromatic polymeric nanofiltration membranes: Extension of Solution-Electro-Diffusion model to complex mixtures, J. Environ. Chem. Eng. 9 (2021) 105262, https://doi.org/10.1016/j.jece.2021.105262.
[16] J. Adusei-Gyamfi, B. Ouddane, L. Rietveld, J.-P. Cornard, J. Criquet, Natural organic matter-cations complexation and its impact on water treatment: a critical review, Water Res 160 (2019) 130–147, https://doi.org/10.1016/j.watres.2019.05.064.
[17] A. Matilainen, E.T. Gjessing, T. Lahtinen, L. Hed, A. Bhatnagar, M. Sillanpää, An overview of the methods used in the characterisation of natural organic matter (NOM) in relation to drinking water treatment, Chemosphere 83 (2011) 1431–1442, https://doi.org/10.1016/j.chemosphere.2011.01.018.
[18] K. Chon, S. Sarp, S. Lee, J.-H. Lee, J.A. Lopez-Ramirez, J. Cho, Evaluation of a membrane bioreactor and nanofiltration for municipal wastewater reclamation: trace contaminant control and fouling mitigation, Desalination 272 (2011) 128–134, https://doi.org/10.1016/j.desal.2011.01.002.
[19] H. Li, Y. Chen, J. Zhang, B. Dong, Pilot study on nanofiltration membrane in advanced treatment of drinking water, Water Supply 20 (2020) 2043–2053, https://doi.org/10.2166/ws.2020.089.
[20] J. Świetlik, E. Sikorska, Application of fluorescence spectroscopy in the studies of natural organic matter fractions reactivity with chlorine dioxide and ozone, Water Res 38 (2004) 3791–3799, https://doi.org/10.1016/j.watres.2004.06.010.
[21] W. Chen, P. Westerhoff, J.A. Leenheer, K. Booksh, Fluorescence excitation-emission matrix regional integration to quantify spectra for dissolved organic matter, Environ. Sci. Technol. 37 (2003) 5701–5710, https://doi.org/10.1021/es034354c.
[22] B. Aftab, J. Cho, H.S. Shin, J. Hur, Using EEM-PARAFAC to probe NF membrane fouling potential of stabilized landfill leachate pretreated by various options, Waste Manag. 102 (2020) 260–269, https://doi.org/10.1016/j.wasman.2019.10.035.
[23] J.A. Korak, A.D. Dotson, R.S. Summers, F.L. Rosario-Ortiz, Critical analysis of commonly used fluorescence metrics to characterize dissolved organic matter, Water Res 49 (2014) 327–338, https://doi.org/10.1016/j.watres.2013.11.025.
[24] C.A. Stedmon, R. Bro, Characterizing dissolved organic matter fluorescence with parallel factor analysis: a tutorial, Limnol. Oceano 6 (2008) 572–579, https://doi.org/10.4319/lom.2008.6.572.
[25] K.R. Murphy, C.A. Stedmon, D. Graeber, R. Bro, Fluorescence spectroscopy and multi-way techniques. PARAFAC, Anal. Methods 5 (2013) 6557–26566, https://doi.org/10.1039/c3ay41160e.
[26] S.V. Jadhav, K.V. Marathe, V.K. Rathod, A pilot scale concurrent removal of fluoride, arsenic, sulfate and nitrate by using nanofiltration: competing ion interaction and modelling approach, J. Process Water Eng. 13 (2016) 153–167, https://doi.org/10.1016/j.jwpe.2016.04.008.
[27] A. Santafé-Moros, J.M. Gozálvez-Zafrilla, J. Lora-García, Performance of commercial nanofiltration membranes in the removal of nitrate ions, Desalination 185 (2005) 281–287, https://doi.org/10.1016/j.desal.2005.02.080.
[28] M. Giagnorio, S. Steffenino, L. Meucci, M.C. Zanetti, A. Tiraferri, Design and performance of a nanofiltration plant for the removal of chromium aimed at the production of safe potable water, J. Environ. Chem. Eng. 6 (2018) 4467–4475, https://doi.org/10.1016/j.jece.2018.06.055.
[29] M.A. Sari, S. Chellam, Relative contributions of organic and inorganic fouling during nanofiltration of inland brackish surface water, J. Membr. Sci. 523 (2017) 68–76, https://doi.org/10.1016/j.memsci.2016.10.005.
[30] J. López, O. Gibert, J.L. Cortina, Evaluation of an extreme acid-resistant sulphonamide based nanofiltration membrane for the valorisation of copper acidic effluents, Chem. Eng. J. 405 (2021) 127015, https://doi.org/10.1016/j.cej.2020.127015.
[31] M.S. Siddique, X. Xiong, H. Yang, T. Maqbool, N. Graham, W. Yu, Dynamic variations in DOM and DBPs formation potential during surface water treatment by ozonation-nanofiltration: using spectroscopic indices approach, Chem. Eng. J. 427 (2022) 132010, https://doi.org/10.1016/j.cej.2021.132010.
[32] Y. Yuan, J.E. Kilduf, Mass transport modeling of natural organic matter (NOM) and salt during nanofiltration of inorganic colloid-NOM mixtures, Desalination 429 (2018) 60–69, https://doi.org/10.1016/j.desal.2017.12.002.
[33] I. Caltran, L.C. Rietveld, H.L. Shorney-Darby, S.G.J. Heijman, Separating NOM from salts in ion exchange brine with ceramic nanofiltration, Water Res 179 (2020) 115894, https://doi.org/10.1016/j.watres.2020.115894.
[34] A. Jurado, E. Vázquez-Suñé, E. Pujades, Potential uses of pumped urban groundwater: a case study in Sant Adrià del Besòs (Spain), Hydrogeol. J. 25 (2017) 1745–1758, https://doi.org/10.1007/s10040-017-1575-3.
[35] O. Coronell, M.I. González, B.J. Mariñas, D.G. Cahill, Ionization behavior, stoichiometry of association, and accessibility of functional groups in the active layers of reverse osmosis and nanofiltration membranes, Environ. Sci. Technol. 44 (2010) 6808–6814, https://doi.org/10.1021/es100891r.
[36] K. Boussu, Y. Zhang, J. Cocquyt, P. Van der Meeren, A. Volodin, C. Van Haesendonck, J.A. Martens, B. Van der Bruggen, Characterization of polymeric nanofiltration membranes for systematic analysis of membrane performance, J. Membr. Sci. 278 (2006) 418–427, https://doi.org/10.1016/j.memsci.2005.11.027.
[37] A. Imbrogno, A.I. Schäfer, Comparative study of nanofiltration membrane characterization devices of different dimension and configuration (cross flow and dead end), J. Membr. Sci. 585 (2019) 67–80, https://doi.org/10.1016/j.memsci.2019.04.035.
[38] A. Zhu, F. Long, X. Wang, W. Zhu, J. Ma, The negative rejection of H^+ in NF of carbonate solution and its influences on membrane performance, Chemosphere 67 (2007) 1558–1565, https://doi.org/:10.1016/j.chemosphere.2006.11.065.
[39] H. Zhao, L. Yang, X. Chen, M. Sheng, G. Cao, L. Cai, S. Meng, C.Y. Tang, Degradation of polyamide nanofiltration membranes by bromine: changes of physiochemical properties and filtration performance, Environ. Sci. Technol. 55 (2021) 6329–6339, https://doi.org/10.1021/acs.est.1c00206.
[40] G. Makdissy, P.M. Huck, M.M. Reid, G.G. Leppard, J. Haberkamp, M. Jekel, S. Peldszus, Investigating the fouling layer of polyamide nanofiltration membranes treating two different natural waters: internal heterogeneity yet converging surface properties, J. Water Supply Res. T. 59 (2010) 164–178, https://doi.org/10.2166/aqua.2010.062.

[41] A. Simon, W.E. Price, L.D. Nghiem, Influence of formulated chemical cleaning reagents on the surface properties and separation efficiency of nanofiltration membranes, J. Membr. Sci. 432 (2013) 73–82, https://doi.org/10.1016/j.memsci.2012.12.029.
[42] C.A. Andersson, R. Bro, The N-way Toolbox for MATLAB, Chemom. Intell. Lab. Syst. 52 (2000) 1–4, https://doi.org/10.1016/S0169-7439(00)00071-X.
[43] N. Pages, A. Yaroshchuk, O. Gibert, J.L. Cortina, Rejection of trace ionic solutes in nanofiltration: influence of aqueous phase composition, Chem. Eng. Sci. 104 (2013) 1107–1115, https://doi.org/10.1016/j.ces.2013.09.042.
[44] M. Reig, E. Licon, O. Gibert, A. Yaroshchuk, J.L. Cortina, Rejection of ammonium and nitrate from sodium chloride solutions by nanofiltration: effect of dominant-salt concentration on the trace-ion rejection, Chem. Eng. J. 303 (2016) 401–408, https://doi.org/10.1016/j.cej.2016.06.025.
[45] I. Puigdomènech, Chemical equilibrium software Hydra and Medusa. Inorganic Chemistry Department, Royal Institute of Technology, Stockholm, Sweden, November 18, 2022. http://w1.156.telia.com/~u15651596/>.
[46] I. Owusu-Agyeman, A. Jeihanipour, T. Luxbacher, A.I. Schäfer, Implications of humic acid, inorganic carbon and speciation on fluoride retention mechanisms in nanofiltration and reverse osmosis, J. Membr. Sci. 528 (2017) 82–94, https://doi.org/10.1016/j.memsci.2016.12.043.
[47] J.K. Park, K.J. Lee, Diffusion coefficients for aqueous boric acid, J. Chem. Eng. Data 39 (1994) 891–894, https://doi-org.recursos.biblioteca.upc.edu/10.1021/je00016a057.
[48] L. Han, J. Tian, C. Liu, J. Lin, J.W. Chew, Influence of pH and NaCl concentration on boron rejection during nanofiltration, Sep. Purif. Technol. 261 (2021) 118248, https://doi.org/10.1016/j.seppur.2020.118248.
[49] Y. Chen, H. Li, W. Pang, B. Zhou, T. Li, J. Zhang, B. Dong, Pilot study on the combination of different pre-treatments with nanofiltration for efficiently restraining membrane fouling while providing high-quality drinking water, Membranes 11 (2021) 380, https://doi.org/10.3390/membranes11060380.
[50] B. Manivannan, M. Borisover, Strengths of correlations with formation of chlorination disinfection byproducts: effects of predictor type and other factors, Environ. Sci. Pollut. Res. 27 (2020) 5337–5352, https://doi.org/10.1007/s11356-019-06976-0.